Optics Letters

Resonant forward scattering of light by high-refractive-index dielectric nanoparticles with toroidal dipole contribution

Pavel D. Terekhov,[1,2,*] Kseniia V. Baryshnikova,[1] Alexander S. Shalin,[1] Alina Karabchevsky,[2] and Andrey B. Evlyukhin[1,3]

[1]ITMO University, 49 Kronversky Ave., 197101, St. Petersburg, Russia
[2]Electrooptical Engineering Unit and Ilse Katz Institute for Nanoscale Science & Technology, Ben-Gurion University, Beer-Sheva 84105, Israel
[3]Laser Zentrum Hannover e.V., Hollerithallee, D-30419, Hannover, Germany
*Corresponding author: terekhovpd@gmail.com

Received 27 December 2016; accepted 14 January 2017; posted 23 January 2017 (Doc. ID 282438); published 13 February 2017

In this Letter, we demonstrate and investigate the Kerker-type effect in high-index dielectric nanoparticles for which the third-order multipoles give a considerable contribution to the light scattering process. It is shown that the Kerker-type effect (strong suppression of the backward light scattering and, simultaneously, resonant forward light scattering) can be associated with the resonant excitation of a toroidal dipole moment in the system. This effect is realized due to the interference of the scattered waves generated by electric, magnetic, and toroidal dipole moments of high-index nanoparticles.

OCIS codes: (290.0290) Scattering; (350.4238) Nanophotonics and photonic crystals; (260.5740) Resonance; (290.4020) Mie theory.

https://doi.org/10.1364/OL.42.000835

Resonant electric and magnetic optical responses in all-dielectric nanostructures attract considerable attention because of their important practical applications [1,2]. These responses are associated with Mie resonances in dielectric nanoparticles with a high refractive index [3]. Recently, these resonances were experimentally demonstrated for spherical nanoparticles made from silicon, which is most commonly used in modern dielectric nanophotonics due to its large dielectric permittivity [4,5]. Dielectric nanoparticles with optical resonant responses can be considered as building blocks for metasurfaces, which can provide efficient control over the phase, amplitude, and directivity of reflected or transmitted light [1,2]. Spectral positions of electric and magnetic multipole resonances of dielectric nanoparticles are determined by their size and aspect ratio [6,7]. This possibility can be used for the realization of the spectral overlap of electric and magnetic dipole resonances resulting in strong suppression of the backward light scattering due to the Kerker effect [8] when the electric and magnetic dipole polarizabilities are equal to each other. In general, strong attenuation of backscattering due to different multipole overlapping may also be related to Kerker-type effects [9]. Directional scattering is very useful for nanophotonics and photovoltaics applications like nanoantennas and metasurfaces [10–12]. Recently the resonant Kerker-type effect has been demonstrated for silicon nanodisks with low aspect ratio (height to diameter) in [13]. Dielectric Huygens' surfaces based on silicon nanodisks have been created and investigated [14].

In contrast to previous works, in this Letter we demonstrate and investigate the realization of the Kerker-type effect in nanoparticles for which the third-order multipoles give a considerable contribution in the light scattering process. As it will be shown, in this case, the Kerker-type effect can be associated with a resonant excitation of a toroidal dipole moment in nanoparticles. Note that the toroidal dipole moment is a Cartesian multipole of the third order and has the same scattered field pattern as an ordinary electric dipole [15]. Recently it has been shown that, due to this property, the contributions of the electric and toroidal dipole moments into scattered fields can compensate for each other (destructive interference), providing total suppression of the electric dipole scattering [16]. This effect was associated with the excitation of the anapole mode in a scatterer [16]. We show that the contributions of electric and toroidal dipole moments into scattered fields can be in phase and interfere constructively, depending on the geometrical parameters of the scatterers, providing resonant enhancement of total electric dipole scattering. In contrast to the anapole state, we propose to call this state a *super-dipole*, because, in this case, the total electric dipole scattering is considerably increased due to the constructive interference between the electric and toroidal dipole moments [15]. A Kerker-type effect in this case can be obtained due to the interference between the electromagnetic fields generated by the toroidal, electric, and magnetic dipole moments.

We consider plane wave scattering by cylindrical silicon nanoparticles with different aspect ratios (Fig. 1). The dielectric permittivity of silicon is taken from [17]. The cylinders' diameter D_c is fixed and is equal to 100 nm, and their height H is ranged between 90 and 300 nm. In contrast to [18], where infinite cylinders were considered, here we consider the frontal plane wave incidence as it is shown in Fig. 1.

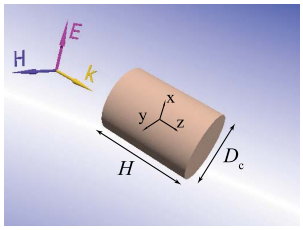

Fig. 1. Cylindrical particle, irradiated by a plane wave, which propagates along the particle's axis. **k** is the wave vector, **E** is the electric field, **H** is the magnetic field, D_c and H are the diameter and the height of the cylinder, respectively.

Our theoretical investigation is based on the multipole decomposition method presented in [15]. Briefly, the regular electric dipole moment of a scatterer is calculated as

$$\mathbf{p} = \int \mathbf{P}(\mathbf{r}')\mathrm{d}\mathbf{r}', \tag{1}$$

where $\mathbf{P}(\mathbf{r}')$ is the polarization induced in the scatterer by an incident light wave and $\mathbf{r}'$ is the radius-vector of a volume element inside the scatterer. The toroidal dipole moment, having the same radiation pattern, is determined as

$$\mathbf{T} = \frac{i\omega}{10}\int \{2\mathbf{r}'^2\mathbf{P}(\mathbf{r}') - (\mathbf{r}'\cdot\mathbf{P}(\mathbf{r}'))\mathbf{r}'\}\mathrm{d}\mathbf{r}'. \tag{2}$$

The expressions for the other multipole moments can be found in [15]. When considering multipole moments up to the electric octupole moment, the scattering cross section can be presented as (see Ref. [15] for details)

$$\begin{aligned}\sigma_{\mathrm{sca}} \simeq{}& \frac{k_0^4}{6\pi\epsilon_0^2|\mathbf{E}_{\mathrm{inc}}|^2}\left|\mathbf{p} + \frac{ik_0\epsilon_d}{c}\mathbf{T}\right|^2 + \frac{k_0^4\epsilon_d\mu_0}{6\pi\epsilon_0|\mathbf{E}_{\mathrm{inc}}|^2}|\mathbf{m}|^2 \\ &+ \frac{k_0^6\epsilon_d}{720\pi\epsilon_0^2|\mathbf{E}_{\mathrm{inc}}|^2}\sum|Q_{\alpha\beta}|^2 + \frac{k_0^6\epsilon_d^2\mu_0}{80\pi\epsilon_0|\mathbf{E}_{\mathrm{inc}}|^2}\sum|M_{\alpha\beta}|^2 \\ &+ \frac{k_0^8\epsilon_d^2}{1890\pi\epsilon_0^2|\mathbf{E}_{\mathrm{inc}}|^2}\sum|O_{\alpha\beta\gamma}|^2,\end{aligned} \tag{3}$$

where k_0 is the free-space wave number; ϵ_0 is the vacuum permittivity; ϵ_d is the relative dielectric permittivity of a surrounding medium (here we consider $\epsilon_d = 1$); μ_0 is the vacuum magnetic permeability; c is the light speed in the vacuum; $\mathbf{E}_{\mathrm{inc}}$ is the electric field amplitude of the incident light wave; **m** is the magnetic dipole moment (MD) of a particle; a term $\mathbf{p} + i\frac{k_0\epsilon_d}{c}\mathbf{T}$ including the interference of electric dipole (ED) and toroidal dipole (TD) moments can be treated as total electric dipole moment (TED); Q, M, and O are the electric quadrupole moment tensor (EQ), the magnetic quadrupole moment tensor (MQ), and the tensor of electric octupole moment (OCT) in irreducible representations, respectively. Note that these tensors are symmetric and traceless [15]. A total scattering cross section is obtained through the integration of the Poynting vector over a closed surface in the far-field zone and the normalization to the incident field intensity [15]. Total electric fields and corresponding induced polarization in scatterers are calculated numerically using COMSOL Multiphysics. Using the calculated polarization, the multipole moments and their contributions into scattering cross sections are obtained by a numerical integration.

Recently, a Kerker-type effect was investigated without the consideration of TD moment contribution [13,19]. We assume that in the particle where this contribution is significant, a Kerker-type effect can be modulated by the toroidal dipole far-field radiation, which is similar to the electric dipole one. In order to estimate the role of different particle multipoles, including the TD moment in the light scattering, first, we show a spectral evolution of the multipole resonances as a function of the nanoparticle size. Figure 2 demonstrates the scattering cross section spectra calculated for nanoparticles of different heights H. One can see that the resonant peaks shift to the red side as H increases [Fig. 2(a)]. Moreover, the spectral distances between these peaks decrease, resulting in a single broad resonant peak for the nanoparticles with $H = 300$ nm [Fig. 2(a)]. Multipole analysis based on Eq. (3) clarifies that these resonance peaks correspond to the overlap of the resonant contributions of several different multipoles. Comparing Figs. 2(a) and 2(b), one can easily see that the single resonant peak at the wavelength of 550 nm for the nanocylinder with $H = 300$ nm combines the resonant contributions from the total electric dipole TED, the magnetic dipole MD, and the magnetic quadrupole MQ [Fig. 2(b)].

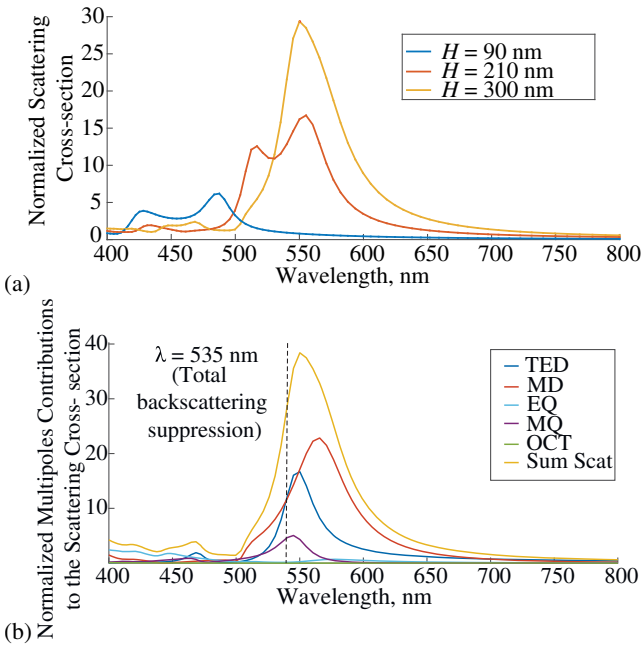

Fig. 2. (a) Scattering cross sections spectra for cylindrical nanoparticles, height $H = 90$ nm (blue line), $H = 210$ nm (red line), and $H = 300$ nm (orange line). (b) Multipole contributions to the scattering cross section spectrum for cylindrical nanoparticle, height $H = 300$ nm. Hereinafter, the values are normalized to the geometric cross section of the cylinder. The black dashed line corresponds to the wavelength of total backscattering suppression (see text below).

It is important that the basic contributions into this resonant peak of the large nanocylinder ($H = 300$ nm, Fig. 2) originate from the total electric and magnetic dipole moments. This is achieved due to the increasing of the TD contribution into the TED moment with the increasing of nanoparticle height. From Fig. 3, demonstrating the absolute value of TED as a superposition of the ED and TD, one can see that, in the case of $H = 90$ nm (the particle aspect ratio is close to 1), the TED is solely determined by the ED contribution in the considered spectral range, whereas for the nanocylinder with

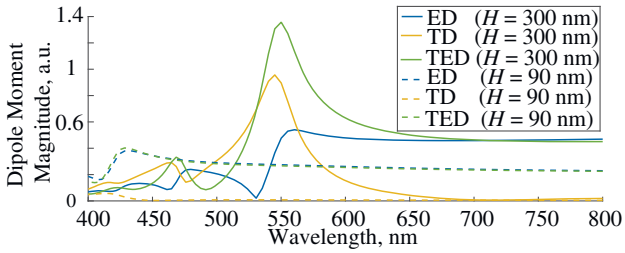

Fig. 3. Spectra of the absolute values of the total electric dipole (TED), the electric dipole (ED), and the toroidal dipole (TD) calculated for the cylindrical nanoparticles with height $H = 300$ nm (solid lines) and $H = 90$ nm (dashed lines).

$H = 300$ nm (the aspect ratio is equal to 3) the TD contribution into the TED is significantly increased, resulting in the strong resonance at the wavelength of ≈550 nm. This resonance state, which is constructive interference (superposition) of the ED and TD moments, corresponds to the *super-dipole* mode mentioned above. Note that the TD moment is a third-order multipole; therefore, its role in the light scattering grows with the increasing of the scatterer size.

According to the Mie theory, spectral positions of multipole resonances for dielectric spherical nanoparticles shift to the red side with the increasing of the nanoparticle size. Spectral distances between different multipole resonances increase as well [20]. In the case of cylindrical nanoparticles, the spectral distances between multipole resonances can be tuned by the changing of a nanoparticle aspect ratio. The spectral evolution of the different multipoles' contributions into the scattering cross sections for the cylindrical nanoparticles as a function of the nanoparticle height H is shown in Fig. 4. It is seen that with the increasing of H (i) the TED [Fig. 4(a)], MD [Fig. 4(b)], and MQ [Fig. 4(c)] resonances grow and shift to the red region because of the increased nanoparticles volumes and (ii) the spectral distances between them decrease due to increasing of the nanoparticles' aspect ratios. As a result, there is a spectral overlap between these resonances at around the 550 nm wavelength for the nanoparticle with $H = 300$ nm [Figs. 2(b) and 4]. The resonant MQ contribution in the total resonant peak in Fig. 4(c) is much smaller than the resonant TED and MD contributions. This is important for the realization of a resonant Kerker-type effect in large-aspect-ratio nanoparticles due to the TED and MD resonances overlap.

Figure 5 shows the normalized forward scattering, determined as an integral of Poynting's vector in the semi-space with z coordinate >0 (here we consider that the external light wave propagates along the positive direction of the z axis and the center of nanoparticles is placed at the origin of the Cartesian system, Fig. 1). The ratio between the forward and backward scattering for the cylindrical nanoparticles with $H = 300$ nm is also shown in Fig. 5. The backward scattering is determined similar to the forward scattering, but with z coordinate <0. From Fig. 5 one can see that the spectral position of the forward scattering maximum corresponds to the maximum of the total scattering cross section [Fig. 2(a)]. However, there is only weak backscattering attenuation at the maximum of the total scattering cross sections (Fig. 5). Much more effective suppression of the backward scattering is realized at the spectral points where the TED contribution to the scattering cross section crosses the MD contribution.

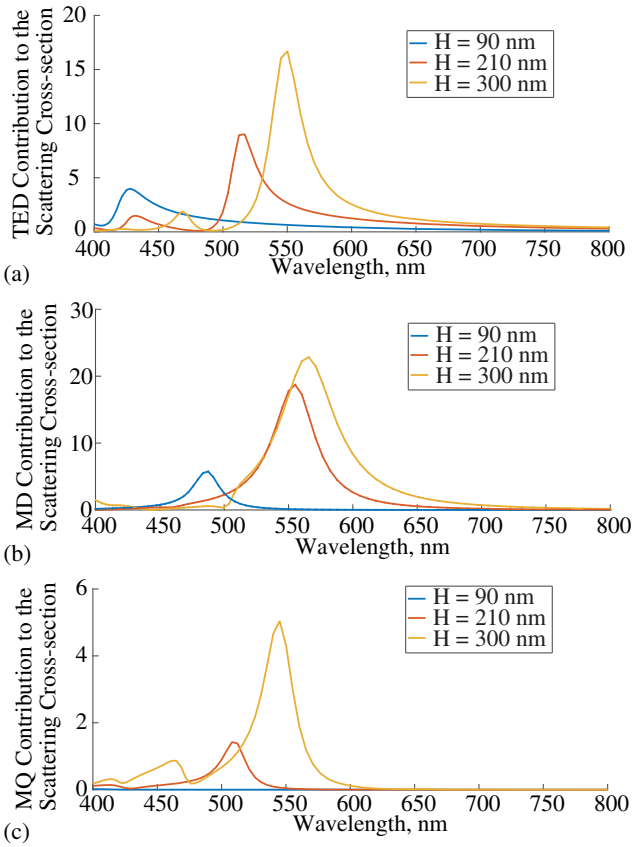

Fig. 4. (a) TED moment, (b) MD moment, and (c) MQ moment contributions to the scattering cross section spectra of the cylindrical nanoparticles of different heights H.

From Fig. 5 it is seen that this is realized in two spectral regions: (i) outside the resonant region for the wavelengths ≳670 nm and (ii) in the resonant region for the wavelength of ≈535 nm. The strong backscattering suppression in the resonant region is connected with resonant excitation of the TD moment, its constructive superposition with the ED moment, and with consequent increasing of the TED. As a result, the destructive (constructive) interference between the fields generated by the MD and TED moments of the scatterer significantly attenuates (enhances) the backward (forward) scattering. Note that in this spectral region the phases of the MD and TED are almost the same (Fig. 6), providing the realization of the Kerker-type effect conditions [8]. Outside the resonant region

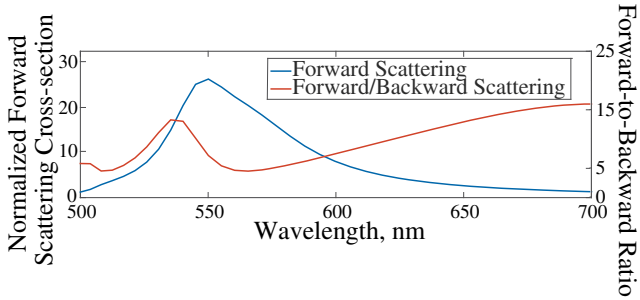

Fig. 5. Forward scattering (blue line) and forward/backward scattering ratio (red line) spectra for cylindrical nanoparticles with $H = 300$ nm.

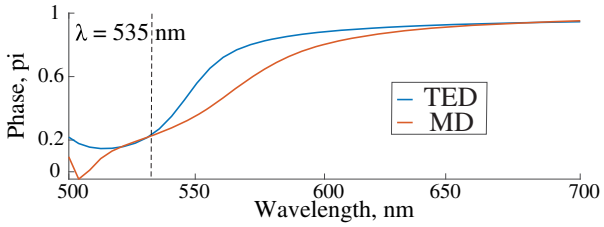

Fig. 6. Phases of the total electric dipole (TED) and the magnetic dipole (MD) calculated for the cylindrical nanoparticle with height $H = 300$ nm.

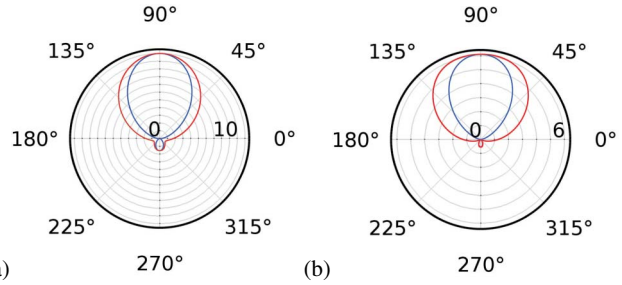

Fig. 7. Scattered field patterns for the silicon cylindrical nanoparticle with $H = 300$ nm, calculated at the wavelength (a) 550 nm and (b) 535 nm. The different colors correspond to the scattered field patterns calculated in the mutually perpendicular planes. The angle of 90° (270°) corresponds to the forward (backward) direction.

(wavelengths $\gtrsim$670 nm), the total scattering is very weak (Fig. 2) and the TD contribution is negligible (Fig. 3). This region corresponds to the realization of a nonresonant backscattering suppression [20].

For an explicit demonstration of the backward scattering suppression, let us consider scattered field patterns for the silicon nanocylinder with height $H = 300$ nm. Figure 7(a) shows the pattern at the wavelength, corresponding to the maximum of the total scattering cross sections [Fig. 2(a) for $H = 300$ nm]. It is seen that the forward scattering (the angle 90° in Fig. 7) is stronger than the backward scattering (the angle 270° in Fig. 7). More significant attenuation of the backward scattering is obtained for the wavelength corresponding to the Kerker-type effect realization. This is clearly demonstrated in Fig. 7(b), where the scattered field pattern is calculated for the resonant maximum of the forward/backward scattering ratio in Fig. 5 (light wavelength = 535 nm). In this case, the backward scattering is suppressed due to the destructive interference between the electromagnetic fields generated by the MD and TED moments, where the main contribution into the TED is provided by the resonant TD moment. The point, corresponding to this Kerker-type effect for the nanocylinder, is marked by a vertical dashed line in Figs. 2(b) and 6.

Additional simulations (not shown here) performed for parallelepipedal nanoparticles show that TD contribution to the realization of Kerker effect is similar to the case of nanocylinders with large aspect ratios. So we assume that aspect ratio is crucial for the considered effect in contrast to a particle concrete form.

In summary, it has been shown, using the multipole decomposition method, that a constructive interference between toroidal and electric dipole moments of the nanoparticle can be realized in silicon nanoparticles. As a result, the total electric dipole moment with a dominant contribution of the toroidal dipole is resonantly excited in the nanoparticles and a so-called super-dipole mode is realized. It has been found that, due to the interference between electromagnetic fields generated by the total electric dipole and magnetic dipole moments of the nanoparticles, the Kerker-type effect (backward scattering suppression) can be realized. Thus our work provides important information about the role of the toroidal dipole moment, resonantly excited in scatterers, in the total and/or directive light scattering by high-index dielectric nanoparticles.

Funding. Russian Foundation for Basic Research (RFBR) (16-52-00112, 17-02-01003); Russian Science Foundation (RSF) (16-12-10287); Deutsche Forschungsgemeinschaft (DFG) (EV 220/2-1); Ministry of Education and Science of the Russian Federation (Minobrnauka) (GOSZADANIE 2014/190).

Acknowledgment. The calculations of multipole moments have been supported by the Russian Science Foundation Grant No. 16-12-10287. A. S. acknowledges the support of the President of Russian Federation in the frame of Scholarship SP-4248.2016.1 and the support of Ministry of Education and Science of the Russian Federation (GOSZADANIE 2014/190). K. B.'s research was partially supported by FASIE. The research described was done as part of a joint Ph.D. program.

REFERENCES

1. A. I. Kuznetsov, A. E. Miroshnichenko, M. L. Brongersma, Y. S. Kivshar, and B. Luk'yanchuk, Science **354**, aag2472 (2016).
2. S. Jahani and Z. Jacob, Nat. Nanotechnol. **11**, 23 (2016).
3. J. A. Stratton, *Electromagnetic Theory* (Wiley, 2007).
4. A. B. Evlyukhin, S. M. Novikov, U. Zywietz, R. L. Eriksen, C. Reinhardt, S. I. Bozhevolnyi, and B. N. Chichkov, Nano Lett. **12**, 3749 (2012).
5. A. I. Kuznetsov, A. E. Miroshnichenko, Y. H. Fu, J. Zhang, and B. Luk'Yanchuk, Sci. Rep. **2**, 492 (2012).
6. A. B. Evlyukhin, C. Reinhardt, and B. N. Chichkov, Phys. Rev. B **84**, 235429 (2011).
7. D. Markovich, K. Baryshnikova, A. Shalin, A. Samusev, A. Krasnok, P. Belov, and P. Ginzburg, Sci. Rep. **6**, 22546 (2016).
8. M. Kerker, D.-S. Wang, and C. Giles, J. Opt. Soc. Am. **73**, 765 (1983).
9. Y. H. Fu, A. I. Kuznetsov, A. E. Miroshnichenko, Y. F. Yu, and B. Luk'yanchuk, Nat. Commun. **4**, 1527 (2013).
10. L. Novotny and N. Van Hulst, Nat. Photonics **5**, 83 (2011).
11. H. A. Atwater and A. Polman, Nat. Mater. **9**, 205 (2010).
12. P. Albella, T. Shibanuma, and S. A. Maier, Sci. Rep. **5**, 18322 (2015).
13. I. Staude, A. E. Miroshnichenko, M. Decker, N. T. Fofang, S. Liu, E. Gonzales, J. Dominguez, T. S. Luk, D. N. Neshev, I. Brener, and Y. S. Kivshar, ACS Nano **7**, 7824 (2013).
14. M. Decker, I. Staude, M. Falkner, J. Dominguez, D. N. Neshev, I. Brener, T. Pertsch, and Y. S. Kivshar, Adv. Opt. Mater. **3**, 813 (2015).
15. A. B. Evlyukhin, T. Fischer, C. Reinhardt, and B. N. Chichkov, Phys. Rev. B **94**, 205434 (2016).
16. A. E. Miroshnichenko, A. B. Evlyukhin, Y. F. Yu, R. M. Bakker, A. Chipouline, A. I. Kuznetsov, B. Luk'yanchuk, B. N. Chichkov, and Y. S. Kivshar, Nat. Commun. **6**, 8069 (2015).
17. E. D. Palik, *Handbook of Optical Constants of Solids* (Academic, 1998), Vol. **3**.
18. W. Liu, A. E. Miroshnichenko, R. F. Oulton, D. N. Neshev, O. Hess, and Y. S. Kivshar, Opt. Lett. **38**, 2621 (2013).
19. S. Campione, L. I. Basilio, L. K. Warne, and M. B. Sinclair, Opt. Express **23**, 2293 (2015).
20. A. B. Evlyukhin, C. Reinhardt, A. Seidel, B. S. Luk'yanchuk, and B. N. Chichkov, Phys. Rev. B **82**, 045404 (2010).